Nordic Pulp & Paper Research Journal Vol 32 no 3, 2017 --- DOI 10.3183/NPPRJ-2017-32-03-p473-482

Characterization of micro-fibrillated cellulose fiber suspension flow using multi scale velocity profile measurements

Markku Kataja, Sanna Haavisto, Juha Salmela, Roope Lehto and Antti Koponen

KEYWORDS: Microfibrillated Cellulose suspension, Optical Coherence Tomography, Ultrasound Velocity Profiling, Rheology, Boundary Layer, Wall Slip.

ABSTRACT: Rheological properties and boundary layer flow behavior of Micro Fibrillated Cellulose (MFC) suspended in water was studied using a novel velocity profiling rheometric technique. The method is based on measuring stationary velocity profiles of fluid flow in a straight tube simultaneously by Doppler Optical Coherence Tomography (DOCT) and by Ultrasound Velocity Profiling (UVP). The high resolution DOCT provides velocity profiles near the transparent tube wall, while UVP yields corresponding information in the interior parts of the flow. The data from the two instruments is combined into a comprehensive velocity profile including both the thin boundary layer near the wall and the interior parts of the flow. Within the boundary layer, concentration and thereby the viscosity of MFC is found to decrease towards the wall. At high flow rate, sublayer of virtually pure water is observed next to the wall, giving rise to apparent wall slip. The results from interior part of the flow show shear thinning behavior in qualitative agreement with results from conventional rheological methods. The results indicate that the new method can provide detailed experimental information on the rheology of MFC suspensions and their intricate boundary layer flow behavior, avoiding uncertainties inherent in many conventional rheological techniques.

ADDRESSES OF THE AUTHORS: Markku Kataja (markku.kataja@jyu.fi) **Roope Lehto** (roope.lehto@jyu.fi), University of Jyväskylä, P.O. Box 35, FI-40014 Jyväskylä, Finland, **Sanna Haavisto** (sanna.haavisto@spinnova.fi) **Juha Salmela** (juha.salmela@spinnova.fi), Spinnova Ltd. Asematie 11, 40800 Vaajakoski, Finland, **Antti Koponen** (antti.koponen@vtt.fi), VTT Technical Research Centre of Finland, P.O. Box 1603, 40101 Jyväskylä, Finland
Corresponding author: Markku Kataja

Introduction

As potential ingredients for novel bio-based materials and high-end products, Microfibrillated Cellulose (MFC) materials are subject of active research and of commercial interest within forest industry. Often, production and processing of MFC involves the fibrous MFC material suspended in a carrier fluid, typically water. Similar to many other natural and synthetic fiber suspensions, the rheological and flow properties of aqueous MFC suspensions are diverse, and depend strongly on the fiber properties and fiber mass concentration (Klemm et al 2011). Already at a very low concentration, aqueous MFC suspensions can show intricate rheological properties such as gel formation, yield stress, shear thinning, hysteresis, and thixotropy (Iotti et al 2011; Karppinen et al 2012; Martoïa et al 2015; Shafiei-Sabet et al 2016; Mohtaschemi et al 2014). These properties derive primarily from the inherent entangled heterogeneous network of fibrils and partially disintegrated fibers having high specific surface area, aspect ratio, strength and flexibility (Lavoine et al 2012).

Conventional experimental techniques for measuring rheological properties of fluids are typically based on simple and well-defined flow geometries where the flow condition is assumed known (Morrison 2001). Analysis of data from such experiments is thus based on certain conjectures concerning the flow velocity profile and boundary conditions that are assumed to prevail in the flow. While appropriate for many homogeneous non-Newtonian fluids, such presumptions are questionable in the case of complex heterogeneous fluids (Mewis, Moldenaers 1999). The rheological parameters thereby obtained may not reflect properties of the fluid alone, but also of the particular flow used in the measurement. Consequently, the parameters may lack generality and lead to erroneous results if applied in flow in conditions not similar to that used in the rheological experiment (Nechyporchuk et al 2014; Saarinen et al 2014; Naderi. Lindström 2016).

The crux of velocity profiling rheometry is to combine conventional rheological techniques and simultaneous measurement of flow velocity profile (Powell et al 1994; Hanlon et al 1998; Raynaud et al 2002; Dogan et. al. 2002; Ouriev, Windhab 2002). The data analysis can then be based on a measured instead of assumed velocity profile. Velocity profiling techniques applicable for turbid fluids are e.g. Nuclear Magnetic Resonance Imaging (NMRI) or Ultrasound Velocity profiling (UVP) (Powell 2008). Both UVP and NMRI have been tested for several rheologically complex fluids and multiphase systems of practical interest e.g. in food, paper and chemical industries (Britton, Callaghan 1997; Dogan et al 2005; Wassell et al 2010; Derakhshandeh et al 2010; Haavisto et al 2011). The concept is well established and has been implemented as in-line rheometers in industrial processes providing means for process monitoring and quality control (Wunderlich, Brunn 1999; Ricci et al 2012; Arola et al 1997; Kotzé et al 2012).

Techniques such as UVP and NMRI allow measuring flow velocity of also turbid fluids well inside the flow. Due to their limited spatial resolution (Manneville 2008; Fock et. al. 2011) and, especially for UVP, disturbance caused by solid-fluid interfaces (Wunderlich and Brunn 2000), these methods are hardly accurate enough to resolve the flow profile in the immediate vicinity of a

Nordic Pulp & Paper Research Journal Vol 32 no 3, 2017 --- DOI 10.3183/NPPRJ-2017-32-03-p473-482

bounding surface. This is unfortunate as the boundary layer behavior of heterogeneous fluids can be quite intricate and can dominate the overall observed flow behavior. A common example of such a case is stationary plug flow of pulp in a straight pipe where the observed velocity is nearly constant in the pipe cross-section and apparent slip occurs at the wall (Pettersson et al 2006; Soszynski 1991; Duffy 2006). Obviously, the complex flow dynamics, reflected e.g. by the measured friction loss behavior of such flow, is dominated by a very thin layer at the tube wall. Obtaining direct experimental data on such a thin layer is not, in general, straightforward for complex flows involving e.g. opaque fluids, and the related flow phenomena remain poorly understood (Fock et al 2011).

Optical Coherence Tomography (OCT) is a non-invasive technique capable of fast real-time high-resolution imaging of the internal structure of an opaque scattering medium in the vicinity of its surface (Fercher et al 2003; Schmitt 1999). The imaging depth of OCT is limited by the used optics and by attenuation of light in the material. In addition to giving access to structural data, the method can be extended to provide velocity information through Doppler Optical Coherence Tomographic (DOCT) technique (Wang et al 1997; Chen, Zhang 2015). Furthermore, the DOCT method appears capable of accurate high-resolution measurement of velocity profile very close to a channel wall, and is thus well suited in detailed study of the boundary layer flow behavior of complex fluids with suitable optical properties (Haavisto et al 2014; Wang 2004; Malm et al 2015).

In this work we report results on rheological and boundary layer flow properties of a MFC suspension, obtained by a novel in-line rheological method (Salmela et al 2013) utilizing velocity profiling. The velocity profile is measured by combining data from simultaneous measurements by DOCT and UVP. Here, DOCT is used to measure the velocity profile in the immediate vicinity of a transparent tube wall, typically closer than 1 mm, while UVP provides the same information in the interior parts of the tube. The combination of data from these instruments provides a comprehensive velocity profile including both the boundary layer and bulk regions of the MFC suspension.

Materials and Methods

Materials

The microfibrillated cellulose used in this work was obtained from Daicel Chemical Industries, Japan. The product type was Celish KY-100G, which is manufactured from purified wood pulp. The basic properties of this commercial MFC have been reported in literature. The average length and diameter of the fibers are 350 μm and 15 μm, respectively (Tatsumi et al 2002). The final MFC suspensions used in the flow experiments were obtained by diluting the original MFC by deionized water to mass concentrations of 0.4%, 1.0% and 1.6% using high intensity mixing by an overhead stirrer (Glas-Col).

Experimental Setup

The measurement unit consisted of a 2.5 m long optical grade glass tube with an inner diameter of 19 mm. The flow in the tube was driven by a low-pulsation progressive cavity pump (Seepex MD series). Total volume of the sample in the flow loop and in the tank was 13.5 liters. The fluid temperature in the loop was set to 21°C with a digital temperature control unit (PolyScience, model 9610). The volumetric flow rate in the loop was adjusted manually using the pump control voltage, and measured using a magnetic flow rate sensor (Siemens, Sitrans F M MAGFLO).

The measurements were carried out at stationary flow conditions at several values of total flow rate in the range 8 – 160 ml/s (see *Fig 3* and *4*). The fluid temperature during each trial point was measured with a thermocouple (Fluke multimeter). The wall shear stress at each flow rate was found based on pressure difference measurement between two 1.5 mm diameter taps drilled through the tube wall located at 74 and 126 diameters downstream from the tube inlet. The pressure difference measurement was done using calibrated sensors (Rosemount, sensor types 3051 and 2051). A schematic of the tube flow system is shown in *Fig 1*.

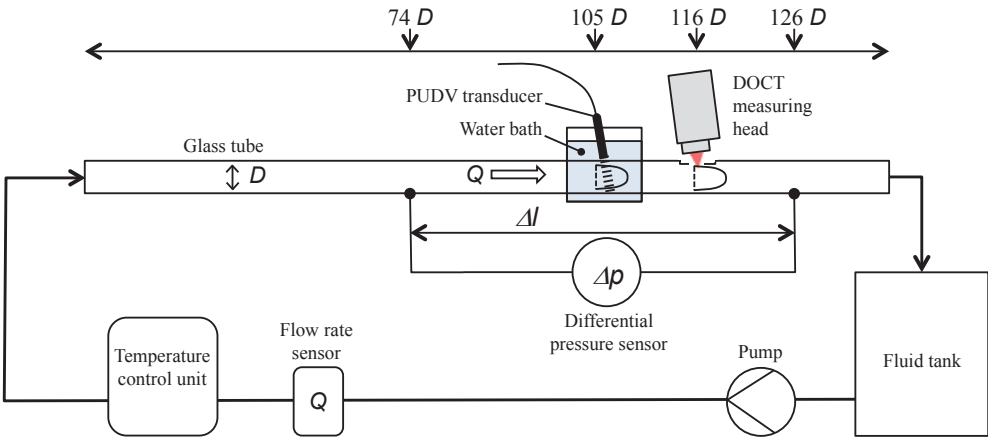

Fig 1- Schematic illustration of the experimental set-up with simultaneous UVP and DOCT measurement of fully developed velocity profile of MFC suspension in a straight glass tube of diameter D=19 mm and length 2.5 m.

Nordic Pulp & Paper Research Journal Vol 32 no 3, 2017 --- DOI 10.3183/NPPRJ-2017-32-03-p473-482

Optical Coherence Tomography

In the spectral domain OCT used in this work, a low coherence light beam is emitted from a super luminescent led light source and split into the sample arm and the reference arm of a Michelson interferometer (Schmitt 1999). The backscattered interference pattern, called A-scan, is Fourier-transformed to give information about the sample scattering index from different depths inside the sample. Cross-sectional images of the sample can be constructed from a series of A-scans by recording depth profiles from different lateral locations of the sample. Such a collection of A-scans is called a B-scan. The resolution of an OCT system in the direction parallel to the light beam is determined by the central wavelength and bandwidth of the light source, while the lateral (cross beam) resolution is determined by the diffraction limited spot size of the focused optical beam. Contrary to standard microscopy, OCT can thereby achieve good parallel resolution independent of the beam focusing and spot size. The OCT device used in this study was Telesto Spectral Domain OCT (Thorlabs, Inc.) with a central wavelength of 1325 nm and bandwidth in excess of 150 nm. The resolutions in the parallel and lateral directions are approximately 3.7 µm (in water) and 15 µm, respectively. The Doppler Optical Coherence Tomography (DOCT) is a modality of OCT that can be used to obtain velocity information. In a DOCT mode, the Doppler frequency generated by a moving object is detected from the phase difference between two or more adjacent A-scans, thus yielding the velocity component in the direction of the light beam (Haavisto et al 2015b).

In this work OCT was used both in imaging the MFC suspension microstructure and for measuring the velocity profile near the tube wall. The OCT measuring head was located 116 tube diameters downstream from the tube inlet. A region of flat surface was ground on the glass tube outer surface in order to minimize thickness of the tube wall and to prevent unwanted refraction of light at the measuring point. In the imaging mode B-scans across a physical width of 5 mm in the tube axial direction were acquired (see *Fig 9*). For flow velocity measurements, small amount of coffee creamer was added as light scattering tracer in the suspension to ensure appropriate level of signal also from the regions of fluid between MFC aggregates. Stationary state velocity profiles at each constant value of flow rate were obtained based on scattering data from a sequence of about 60 000 A-scans at a single position. The data acquisition frequency was 5.5, 28 or 91 kHz, depending on flow rate. Assuming fully developed flow in the tube, the axial velocity profile is given by

$$u(y) = \frac{u_b(y)}{\cos\theta_D}, \qquad [1]$$

where y is the distance from the tube wall, $u_b(y)$ is the measured velocity component in the beam direction and θ_D is the Doppler angle (angle of the incident light beam and tube axis). The value of the Doppler angle was conveniently obtained by utilizing the imaging modality of OCT at the same setting of the measuring probe, and evaluating the inclination of the tube inner wall visible in the images (see *Fig. 9*). A typical value of θ_D used here was 86° – 87°.

Ultrasound Velocity Profiling

Ultrasound velocity profiling technique is based on using an emitter/receiver to send a series of short ultrasound bursts into the flow, and detecting the sound reflected from the target particles moving along with the flow. The location of the particles is acquired with the time-of-flight method using the known velocity of sound. The velocity of the moving particles is calculated from cross-correlation between the echoes from consecutive pulses. In the present study, a DOP2000 (Signal-Processing S.A., Switzerland) device equipped with an 8 MHz ultrasound probe was used. The probe was installed in a water bath surrounding the tube 105 diameters downstream from the tube inlet, and at angle of 78.5° relative to tube axis. The pulse repetition frequency was varied between 500 and 2000 Hz in order to exploit full velocity resolution range. The pulse length was ~0.38 mm in water (2 wavelengths), which also gives the spatial resolution. In all measurements, 32 consecutive pulse emissions were used to calculate a single velocity value in each sampled depth locations. The mean velocity profile for a given flow rate was calculated as the average of the results from 500 individual velocity profiles measurements.

In analogy to DOCT, the present UVP device measures a single velocity component in the direction of the ultrasound beam. The flow velocity u is again given by *Eq 1*, and is thus susceptible to systematic error related to uncertainty in the value of θ_D ($\lesssim$90°). The Doppler angle for the UVP measurement was determined manually by measuring the setting angle between the tube upper surface and the body of the ultrasound transducer. Here, error may occur as the actual Doppler angle, i.e. the angle of incident of the ultrasound beam that enters the flow, may deviate from the measured probe setting value due to e.g. mechanical manufacturing tolerances of the probe, angle measurement error and refraction of sound at tube wall surfaces. Similar uncertainty applies also to DOCT although in that case, the Doppler angle can be found more directly using the imaging mode of OCT, as discussed above. More detailed discussion on the effects of various uncertainties related to the two methods can be found in reference (Szkulmowska et al 2008; Messer, Aidun 2009).

Results and Discussion

In *Fig 2 (a)* shown is the measured pressure loss as a function of flow rate measured in a straight tube of diameter D=19 mm at various values of concentration of MFC suspension. The pressure loss behavior is found to be qualitatively similar to that of pseudoplastic fluids. At the lowest concentration of 0.4%, the non-linear behavior is quite weak, however. At the highest concentration of 1.6% instead, the pressure loss shows a distinct plateau, similar to what is often found for e.g. pulp suspensions (Jäsberg 2007; Sumida 2013; Duffy 2006). The detailed reason for such behavior is discussed below.

Nordic Pulp & Paper Research Journal Vol 32 no 3, 2017 --- DOI 10.3183/NPPRJ-2017-32-03-p473-482

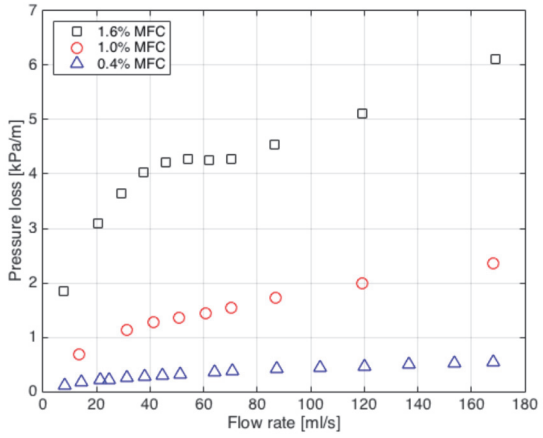

(a)

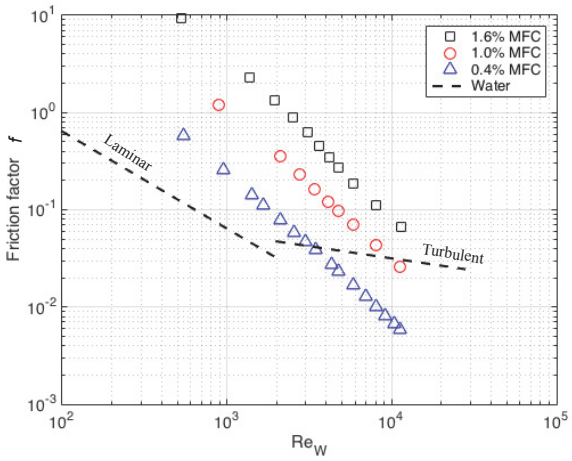

(b)

Fig 2 - (a) Measured pressure loss vs. flow rate for MFC suspension at various concentrations. (b) Friction factor vs. Reynolds number calculated using viscosity of water. Also shown are the standard correlations for water in laminar flow (f = 64/Re) and in turbulent flow for smooth pipes according to Blasius' correlation (f = 0.316/Re$^{0.25}$).

Fig 2(b) shows the loss behavior in terms of Darcy friction factor as a function of Reynolds number Re_w calculated using viscosity of water. The data does not show evidence on transition to turbulent flow in the used range of flow rate. Especially in the case of 0.4% consistency the delayed transition to turbulence leads to distinct drag reduction typical to many polymer solutions and fiber suspensions (Escudier et al 1999; Lee, Duffy 1976).

Velocity Profiles

In most cases studied in this work, the velocity profiles measured by DOCT in the near wall region and by UVP in the interior parts of the tube show overlapping region of mutually consistent results. Typically, such overlap region is found within distance 0.5 – 1.0 mm from the tube wall, see *Fig 3 (a)* and *(b)*. Slight systematic deviation may occur e.g. due to the uncertainty of the used values of Doppler angle. In practice, appropriate match in the overlap region was thus achieved by fine-tuning the Doppler angle used in *Eq 1* for the UVP measurement. The combined velocity profile was then normalized such that the integrated total flow rate coincides with the flow rate measured independently by the magnetic flow rate sensor. This procedure of matching and normalization of the velocity profiles helps eliminating the systematic uncertainties related to absolute velocity values inherent in both methods while retaining the information related to the shape of the profiles. In the case of MFC at concentration 1.6%, the penetration depth of the DOCT light signal was reduced and the regions of accurate measurement of the two techniques do not show distinct overlap (see *Fig 3 (c)*). In this case reasonably accurate patching of the profiles was nevertheless obtained by using DOCT results extrapolated into the UVP measurement region by means of a suitable fitting function (see *Eq 3* below). In all measured cases, the corrections to the measured UVP Doppler angle required for profile matching and to the overall flow rate normalization, were below 0.3° and 10%, respectively.

Fig 3 shows the combined stationary velocity profiles at various total flow rates, as measured with DOCT and UVP techniques. (The bulge present in the velocity profile for the highest flow rate in *Fig 3(a)* is most likely a measurement error. Such artifacts are typically created by spurious reflections of the ultrasound pulses from tube walls, air bubbles etc.) The overall velocity profile appears to include two dynamically different parts. In the interior part of the tube, at the distance range of 200 µm $\lesssim y \leq D/2$, the profile is relatively shallow and qualitatively resembles that of a pseudoplastic fluid. In macroscopic scales the flow behavior of MFC appears as that of a shear thinning fluid with wall slip. The high-resolution DOCT data shown in more detail in *Fig 4* reveals, however, that in a thin near-wall region, the velocity profile is very steep and approaches rapidly zero towards the wall. No actual wall slip is thus observed.

Viscosity Characteristics

Given the combined velocity profile $u(y)$ it is straightforward to numerically estimate the value of local shear rate $\dot{\gamma} = du(y)/dy$ at distance y from the wall. For a stationary axial flow, the shear stress at position y is given by $\tau(y) = \tau_w(1 - y/R)$, R is tube radius and $\tau_w = R\Delta p/2L$ is the wall shear stress obtained from pressure loss Δp measured over a tube segment of length L (here 54 pipe diameters). The local value of viscosity at position y is thus given by

$$\mu(y) = \frac{\tau(y)}{\dot{\gamma}(y)}. \qquad [2]$$

Utilizing the measured velocity profile we thus obtain the viscosity profile within the entire range of shear rate values present in the flow at each constant total flow rate. Notice however, that for MFC materials studied here, the total shear stress $\tau(y)$ may include elastic contribution. The viscosity formally defined by *Eq 2* may thus not be purely of frictional origin, and may depend on elastic strain in addition to strain rate.

Nordic Pulp & Paper Research Journal Vol 32 no 3, 2017 --- DOI 10.3183/NPPRJ-2017-32-03-p473-482

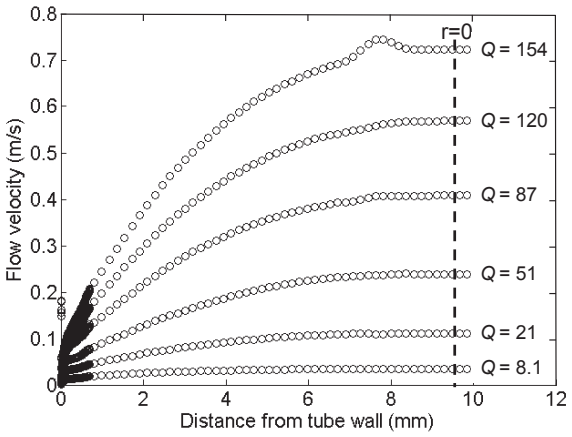

(a) MFC 0.4%

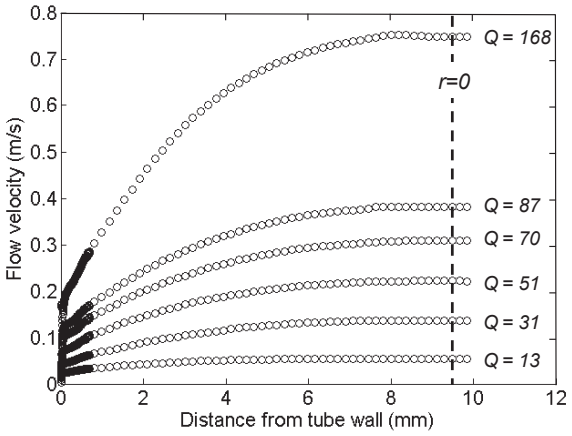

(b) MFC 1.0%

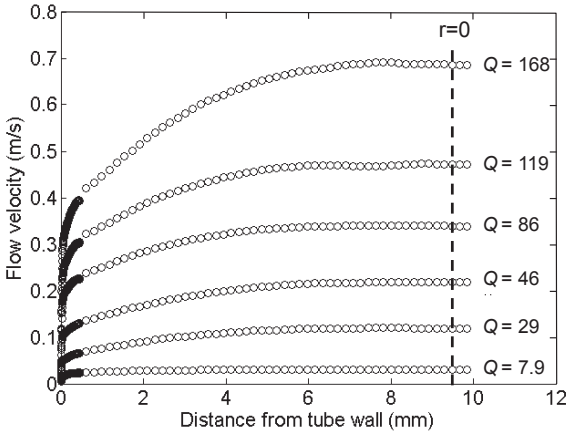

(c) MFC 1.6%

Fig 3 - Velocity profiles of three different MFC suspensions combined from DOCT and UVP measurements. The velocity values from DOCT, appearing as dark symbols near the wall, are shown in more detail in *Fig 4*. The labels to different profiles give the total low rate [ml/s]. The vertical dashed line indicates centerline of the tube.

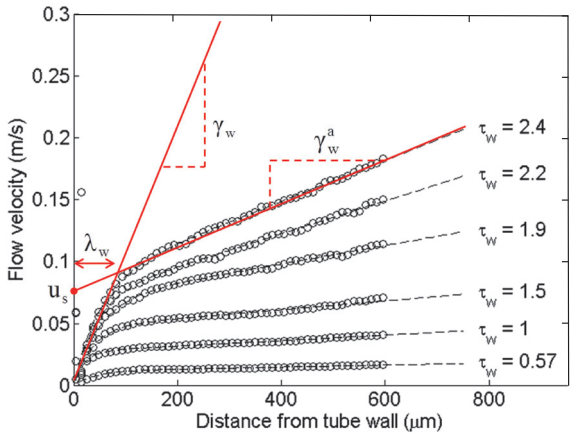

(a) MFC 0.4%

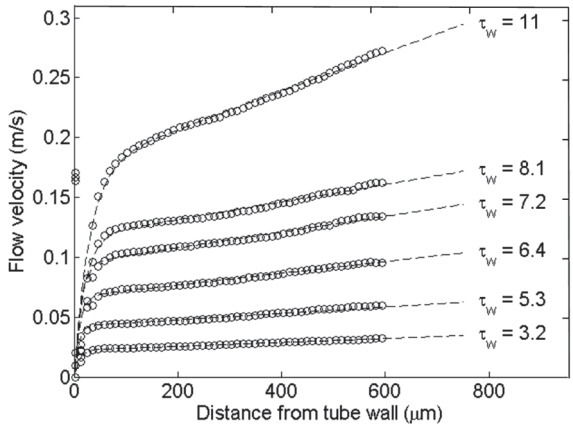

(b) MFC 1.0%

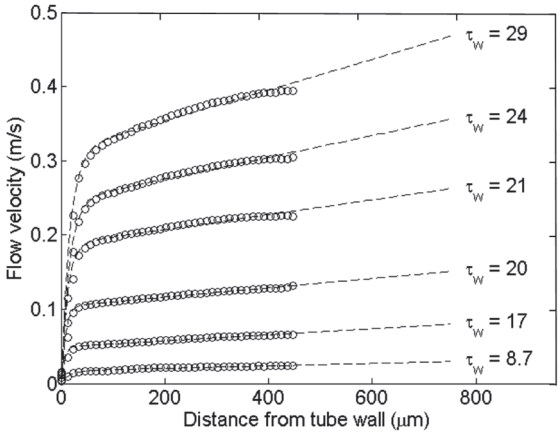

(c) MFC 1.6%

Fig - 4. Near-wall velocity profiles measured by DOCT. The labels to different profiles give the wall stress [Pa] (the corresponding flow rates can be found in *Fig 3*). Graphs of *Eq 3* fitted to DOCT data are shown as dashed lines. The geometric interpretation of the fitting parameters is given in subfigure (a)

Nordic Pulp & Paper Research Journal Vol 32 no 3, 2017 --- DOI 10.3183/NPPRJ-2017-32-03-p473-482

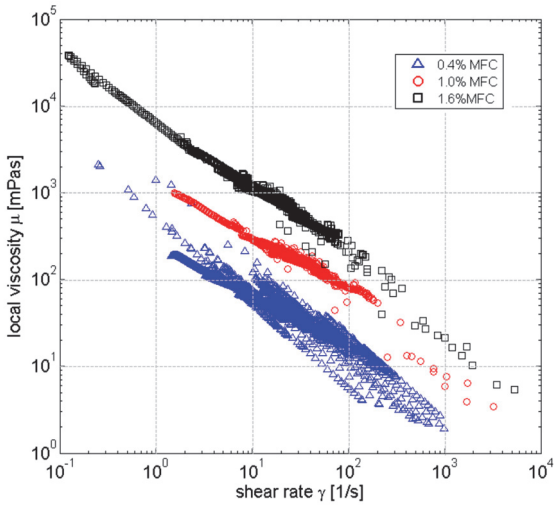

Fig 5 - Viscosity of MFC suspensions at various concentrations as a function of shear rate, calculated locally from the measured velocity profiles.

Fig 5 summarizes the values of viscosity vs. shear rate, obtained from *Eq 2*, for all values of flow rate measured and for the three values of consistency. The viscosity behavior of MFC suspension shows overall shear-thinning characteristics, in qualitative accordance with results obtained with conventional rheometric techniques (Haavisto et. al. 2015a; Kumar et. al. 2016; Agoda-Tandjawa et. al. 2010; Saarinen et. al. 2014).

At low values of shear rate ($\dot{\gamma} \lesssim 10$ s^{-1}), originating from inner parts of the tube, the measured values of viscosity show power-law type of correlation with shear rate. At higher values of shear rate, related to the near-wall boundary layer, the behavior is qualitatively different, as viscosity does not show clear correlation with shear rate alone. Indeed, closer examination of the boundary layer, discussed in more detail in the next section, indicates that concentration of MFC decreases towards the wall in that thin layer. Within the boundary layer viscosity thus depends on both the local shear rate and the local concentration, and can have values significantly lower than in the interior parts of the tube.

Boundary Layer Behavior

We now study the boundary layer behavior and the rheological properties of MFC suspension near the tube wall using the DOCT data shown in *Fig 4*. Within the region $y \lesssim 500$ μm, the measured velocity profiles can be closely approximated by the formula

$$u(y) = \dot{\gamma}_w^a y + u_s^a\left(1 - e^{-y/\lambda_w}\right), \qquad [3]$$

where λ_w, u_s^a, and γ_w^a are free parameters found by fitting to the velocity profile data. The parameter λ_w characterizes the thickness of the wall boundary layer underlying the apparent wall slip. The parameters u_s^a and γ_w^a can be interpreted as the apparent slip velocity and the apparent wall shear rate, respectively (see *Fig 4 (a)*). Using these parameters, we can also define the apparent value of viscosity at wall as $\mu_w^a = \tau_w/\dot{\gamma}_w^a$. As obvious from these definitions the term 'apparent' is used here to refer to wall quantities observable in the macroscopic scales and related to the velocity profile shape just outside the boundary layer ($y \gtrsim \lambda_w$). In principle, the apparent parameters could be measured using UVP or similar low-resolution technique alone. Instead, measuring the boundary layer thickness and the velocity profile within the thin boundary layer require high-resolution method such as DOCT.

The shear rate at the wall ($y = 0$) is given in terms of the three fitting parameters described above as

$$\dot{\gamma}_w \equiv \left(\frac{du}{dy}\right)_{y=0} = \dot{\gamma}_w^a + \frac{u_s^a}{\lambda_w} \quad . \qquad [4]$$

The value of viscosity at wall is then given by $\mu_w = \tau_w/\dot{\gamma}_w$. As evident from the shape of the velocity profiles shown in *Fig 4*, we typically have that $\dot{\gamma}_w \gg \dot{\gamma}_w^a$, and thus that $\mu_w \ll \mu_w^a$ and $\dot{\gamma}_w \approx u_s^a/\lambda_w$.

Fig 6 shows the measured wall shear stress and the apparent viscosity at wall as functions of apparent wall shear rate for the MFC suspensions at various concentrations. Again, we notice that the overall behavior of the suspension is shear thinning and, especially at the lower values of consistency, is qualitatively close to that of a power law fluid for which $\tau \propto \dot{\gamma}^{\frac{1}{2}}$ $\left(\mu \propto \dot{\gamma}^{-\frac{1}{2}}\right)$.

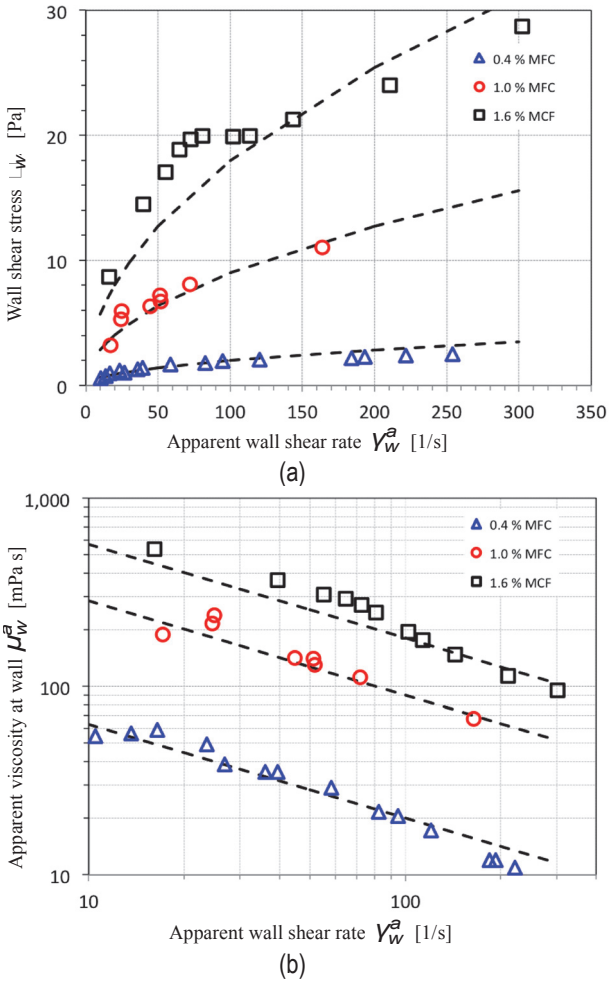

Fig 6 - Wall shear stress (a) and apparent viscosity (b) at wall as functions of apparent shear rate at wall for MFC suspension at various values of consistency. The dashed lines representing power law behavior $\tau \propto \dot{\gamma}^{\frac{1}{2}}$ are shown for reference.

Nordic Pulp & Paper Research Journal Vol 32 no 3, 2017 --- DOI 10.3183/NPPRJ-2017-32-03-p473-482

The plateau visible in the shear stress behavior of especially 1.6% MFC (see also *Fig 2(a)*) is most likely related to existence of concentration gradient and, at higher values of flow rate, even of a thin particle depletion layer near the wall. The well-known explanation for such phenomenon is given by the combined effect of steric hindrance and repulsive hydrodynamic interaction between the tube wall and suspended particles (Barnes 1995; Medhi et al 2011; Leighton, Acrivos 1987; Jäsberg et al. 2000). This interpretation is supported by *Fig 7 (a)* and *(b)* showing the measured dependence of viscosity at wall and of apparent slip velocity on wall shear stress, respectively. At low values of wall shear stress (and of flow rate), viscosity at wall decreases and slip velocity increases with wall shear stress. In the case of 1.6% MFC a distinct transition at $\tau_w \approx 20$ Pa is found. Around that point, apparent slip velocity increases rapidly while viscosity at wall becomes constant with the value near that of water ($\mu_w \sim$ 1 mPa·s). A plausible interpretation of this result is that at low flow rate, the particulate phase is in contact with tube wall, and contributes to total friction. The repulsive hydrodynamic force between the tube wall and the particles increases with flow rate leading to gradual decrease of elastic normal force and of direct friction between particles and the wall.

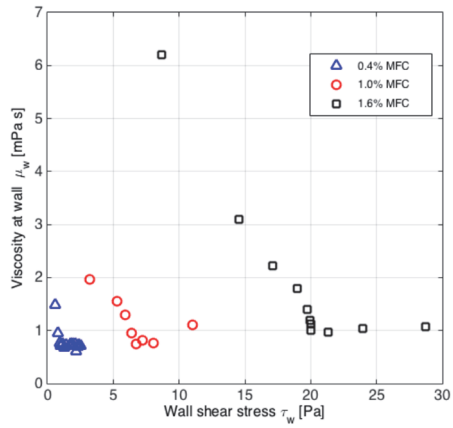

(a)

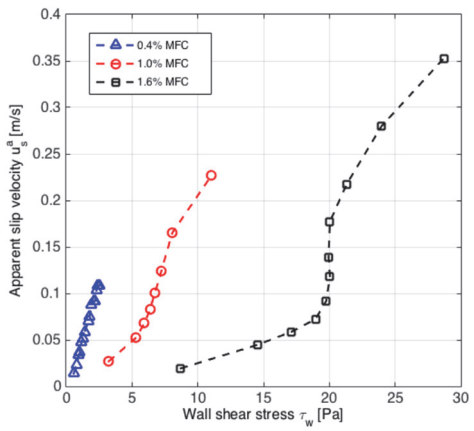

(b)

Fig 7 - Viscosity at tube wall $y = 0$ (a) and apparent slip velocity (b) as functions of wall shear stress for MFC suspension at various concentrations.

In the transition point, repulsive interaction overcomes the elastic stress in the MFC material and a narrow layer of virtually pure water is formed near the wall. Such an effect characterizes also flows of *e.g.* pulp suspensions (Derakhshandeh et al 2011). In the case of 1.0% MFC similar but somewhat less abrupt transition occurs at $\tau \approx$ 7 Pa. At the lowest consistency of 0.4%, the transition seems to occur already at very low flow rate, being barely visible in the viscosity behavior shown in *Fig 7 (a)*. The increase of the transition point and the more distinct characteristics of the transition are qualitatively explained by the increase of elastic stiffness of the fibrous network with consistency of the MFC material.

The existence of the low viscosity layer is visible also in *Fig 8* showing the local values of viscosity for consistency 1.0% as a function of distance from the wall, for several values of total flow rate. The local values of viscosity are obtained from *Eq 2* and *3* using the measured values of wall shear stress τ_w and parameters λ_w, u_s^a, and γ_w^a fitted to DOCT velocity profiles shown in *Fig 4(b)*. Outside of the boundary layer viscosity decreases with flow rate (and with local shear rate). Towards the wall, the value of viscosity decreases and approaches that of water irrespective of the flow rate, and thus, of the wall shear rate. Direct qualitative evidence on correlation between viscosity behavior and concentration gradient near the wall is obtained by utilizing the imaging modality of OCT. *Fig 9* shows examples of still images of the structure of MFC suspension flow near the tube wall together with long time averaged images. The OCT images are constructed as the spatial distribution of back-scattering index of light. The scattering index, in turn, correlates with the concentration of suspended particles that contribute to scattering. The light shades of grey near the tube wall thus indicate lower concentration as compared to inner parts of the tube. The concentration boundary layer is barely visible in the case of 1.6% MFC. More detailed study of the correlation between concentration and viscosity will be presented elsewhere.

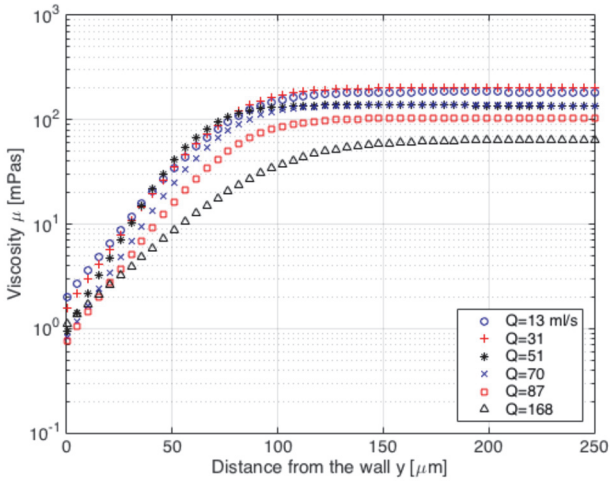

Fig 8 - Viscosity of 1.0% MFC suspension as a function of distance from the wall for several values of total flow rate. The local values of viscosity are calculated based on measured wall shear stress and on velocity profiles fitted to DOCT data.

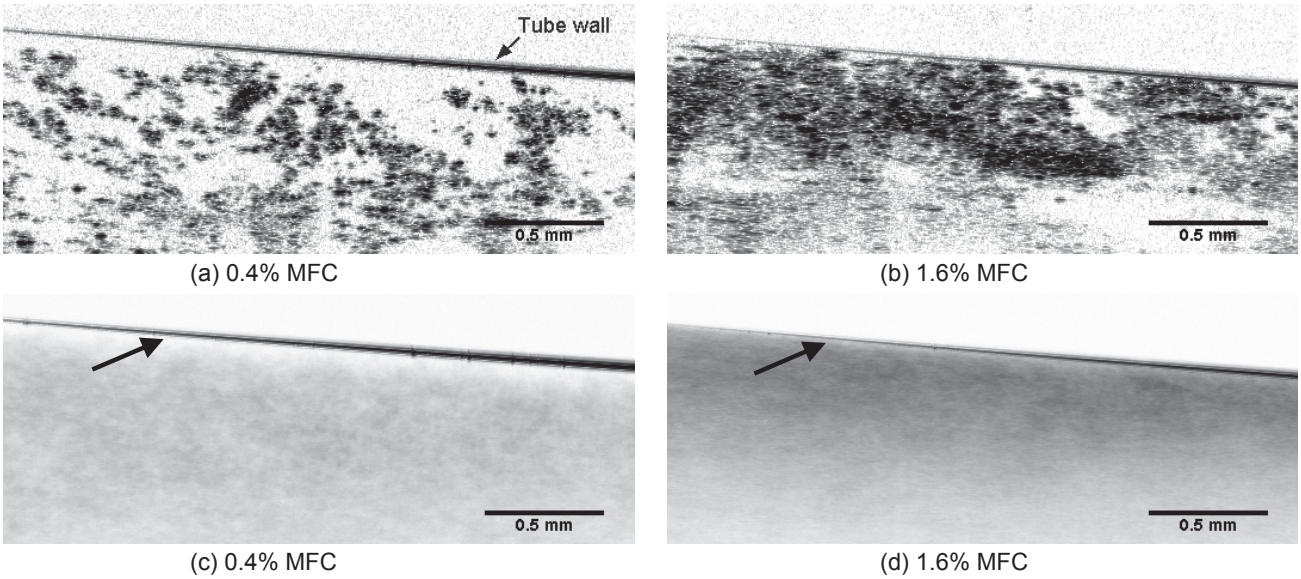

(a) 0.4% MFC (b) 1.6% MFC

(c) 0.4% MFC (d) 1.6% MFC

Fig 9 - OCT still images (a-b) and long time average images (c-d) of boundary layer flow of MFC suspension of consistencies 0.4% and 1.6%. The regions covered by MFC and water are shown in the still images as dark and light gray shades, respectively. The time averaged images are obtained as mean of 200 still images taken over a time interval of about 20 s. The boundary layer with concentration decreasing towards the tube wall appears as lighter gray color and is indicated by arrows in subfigures (c) and (d). The apparent inclination of the tube wall in the images is due to setting angle of the DOCT measuring head, as required for axial velocity measurement.

Conclusions

A novel experimental method, based on simultaneous use of Doppler Optical Coherence Tomography (DOCT) and Ultrasound Velocity Profiling (UVP), was used to study the rheological properties and boundary layer behavior of micro-fibrillated cellulose (MFC) suspension flow in a straight tube at consistencies 0.4%, 1.0%, and 1.6% by weight. The two velocity profiling methods are complementary in the sense the DOCT technique is capable of high-resolution measurement of the boundary layer flow very close to the tube wall while the UVP method is useful in measuring the velocity profile in the interior parts of the tube with lower spatial resolution. A comprehensive velocity profile including both the thin boundary layer and the interior parts of the tube can be obtained by combining the velocity profiles from the two methods. Such combination is straightforward at lower values of consistency where the effective measuring ranges of the two methods overlap. At consistency 1.6% the penetration depth of the optical signal of DOCT was reduced such that no distinct overlap was achieved. Even then, adequate patching of the profiles was obtained by slight extrapolation of the measured results.

In the interior parts of the tube where the MFC consistency is constant, in average, the results show typical shear thinning behavior, in qualitative agreement with results obtained by conventional rheometric methods. The near wall behavior shows existence of a boundary layer where the mean concentration decreases towards the wall. Such a concentration gradient is most likely created by combined effect of steric hindrance by the wall and hydrodynamic lift that induces migration of MFC particles away from the wall. The thickness of such boundary layer increases with flow rate and decreases with MFC concentration. The maximum boundary layer thickness observed here was of the order of 200 μm. With increasing flow rate (wall shear stress), the fluid next to the tube wall may become nearly Newtonian with viscosity close to that of water. Such behavior indicates existence of a sublayer depleted of particles in the close vicinity of the wall, and leads to apparent wall slip. The local value of viscosity increases with distance from the wall, along with increasing concentration. The concentration boundary layer can be directly observed by using the imaging modality of optical coherence tomography.

Acknowledgements

This work was part of the project Rheology of Complex Fluids funded by the Academy of Finland. This project has received funding also from the European Union's Horizon 2020 research and innovation programme under grant agreement No 713475 (Spinnova Ltd). The experiments were carried out in a laboratory facility of University of California in Davis, Department of Food Science and Technology, and were supported by EU COST Action FP1005. The authors highly appreciate collaboration with UC Davis, in particular with professor Michael J. McCarthy and professor Robert L. Powell.

References

Agoda-Tandjawa G., Durand S., Berot S., Blassel C., Gaillard C., Garnier C. and Doublier J.-L. (2010): Rheological characterization of microfibrillated cellulose suspensions after freezing, Carbohydr. Polym. 80(3), 677-686.

Arola D. F., Barrall G. A., Powell R. L., McCarthy M. J. and McCarthy K. L. (1997): Use of nuclear magnetic resonance imaging as a viscometer for process monitoring, Chem. Eng. Sci. 52(13), 2049-2057.

Barnes H. A. (1995): A review of the slip (wall depletion) of polymer solutions, emulsions and particle suspensions in viscometers: its cause, character, and cure, J. Non Newtonian Fluid Mech. 56(3), 221-251.

Britton M. M. and Callaghan P. T. (1997): NMR microscopy and the non□linear rheology of food materials, Magn. Reson. Chem. 35(13)

Chen Z and Zhang J (2015):. "Doppler optical coherence tomography,"Optical Coherence Tomography: Technology and Applications, eds. W. Drexler and J. G. Fujimoto Switzerland: Springer, 1289-1320

Derakhshandeh B., Kerekes R., Hatzikiriakos S. and Bennington C. (2011): Rheology of pulp fibre suspensions: A critical review, Chem. Eng. Sci. 66(15), 3460-3470.

Derakhshandeh B., Hatzikiriakos S. G. and Bennington C. P. (2010): Rheology of pulp suspensions using ultrasonic Doppler velocimetry, Rheologica Acta 49(11-12), 1127-1140.

Dogan N., McCarthy M. and Powell R. (2002): In□Line Measurement of Rheological Parameters and Modeling of Apparent Wall Slip in Diced Tomato Suspensions Using Ultrasonics, J. Food Sci. 67(6), 2235-2240.

Dogan N., McCarthy M. J. and Powell R. L. (2005): Measurement of polymer melt rheology using ultrasonics-based in-line rheometry, Meas. Sci. Technol. 16(8), 1684-1690.

Duffy G. G. (2006): Measurements, mechanisms and models: Some important insights into the mechanisms of flow of fibre suspensions, Annual Transactions of The Nordic Rheology Society 14, Nordic Rheology Society, ,19-31.

Escudier M., Presti F. and Smith S. (1999): Drag reduction in the turbulent pipe flow of polymers, J. Non Newtonian Fluid Mech. 81(3), 197-213.

Fercher A. F., Drexler W., Hitzenberger C. K. and Lasser T. (2003): Optical coherence tomography - principles and applications, Reports on Progress in Physics 66(2), 239-303.

Fock H., Claesson J., Rasmuson A. and Wikström T. (2011): Near wall effects in the plug flow of pulp suspensions, TCan. J. Chem. Eng. 89(5), 1207-1216.

Haavisto S., Lille M., Liukkonen, J., Jäsberg, A., Koponen A. and Salmela J. (2011): Laboratory-Scale Pipe Rheometry: A Study of a Microfibrillated Cellulose Suspension, Proceedings of Papercon 2011, Northern Kentucky Convention Center, May 1-4, Proceedings of Papercon 2011, ,357-370.

Haavisto S., Salmela J., Jasberg A., Saarinen T., Karppinen A. and Koponen A. (2015a): Rheological characterization of microfibrillated cellulose suspension using Optical Coherence Tomography, Tappi J. 14(5), 291-302.

Haavisto S., Salmela J. and Koponen A. (2015b): Accurate velocity measurements of boundary-layer flows using Doppler optical coherence tomography, Exp. Fluids 56(5), 1-6.

Haavisto S., Koponen A. I. and Salmela J. (2014): New insight into rheology and flow properties of complex fluids with Doppler optical coherence tomography, Front. Chem. 2(27), 1-6.

Hanlon A. D., Gibbs S. J., Hall L. D., Haycock D. E., Frith W. J. and Ablett S. (1998): Rapid MRI and velocimetry of cylindrical couette flow, Magn. Reson. Imaging 16(8), 953-961.

Iotti M., Gregersen Ø W., Moe S. and Lenes M. (2011): Rheological Studies of Microfibrillar Cellulose Water Dispersions, J. Polym. Environ. 19(1), 137-145.

Jäsberg A (2007): Flow Behaviour of Fibre Suspensions in Straight Pipes: New Experimental Techniques and Multiphase Modeling, Ph.D. Thesis, University of Jyväskylä, Jyväskylä, Finland.

Jäsberg A., Koponen A., Kataja M. and Timonen J. (2000): Hydrodynamical forces acting on particles in a two-dimensional flow near a solid wall, Comput. Phys. Commun. 129(1), 196-206.

Karppinen A., Saarinen T., Salmela J., Laukkanen A., Nuopponen M. and Seppälä J. (2012): Flocculation of microfibrillated cellulose in shear flow, Cellulose 19(6), 1807-1819.

Klemm D., Kramer F., Moritz S., Lindström T., Ankerfors M., Gray D. and Dorris A. (2011): Nanocelluloses: A new family of nature□based materials, Angew. Chem Int. Ed. 50(24), 5438-5466.

Kotzé R., Wiklund J. and Haldenwang R. (2012): Optimization of the UVP+PD rheometric method for flow behavior monitoring of industrial fluid suspensions, Applied Rheology 22(4), 42760-42761.

Kumar V., Nazari B., Bousfield D. and Toivakka M. (2016): Rheology of microfibrillated cellulose suspensions in pressure-driven flow, Applied Rheology 55, 3603-3613.

Lavoine N., Desloges I., Dufresne A. and Bras J. (2012): Microfibrillated cellulose - its barrier properties and applications in cellulosic materials: a review, Carbohydr. Polym. 90(2), 735-764.

Lee P. and Duffy G. (1976): Analysis of the drag reducing regime of pulp suspension flow, Technical Association of Pulp & Pap Ind, Jour of 59(8)

Leighton D. and Acrivos A. (1987): The shear-induced migration of particles in concentrated suspensions, J. Fluid Mech. 181, 415-439.

Malm A., Waigh T., Jaradat S. and Tomlin R. (2015): Optical coherence tomography velocimetry with complex fluids, JJ. Phys. Conf. Ser. 602(1), 012039-012045.

Manneville S. (2008): Recent experimental probes of shear banding, Rheologica Acta 47(3), 301-318.

Martoïa F., Perge C., Dumont P., Orgéas L., Fardin M., Manneville S. and Belgacem M. (2015): Heterogeneous flow kinematics of cellulose nanofibril suspensions under shear, Soft Matter 11(24), 4742-4755.

Medhi B. J., Kumar A. A. and Singh A. (2011): Apparent wall slip velocity measurements in free surface flow of concentrated suspensions, Int. J. Multiphase Flow 37(6), 609-619.

Messer M. and Aidun C. K. (2009): Main effects on the accuracy of Pulsed-Ultrasound-Doppler-Velocimetry in the presence of rigid impermeable walls, Flow Meas. Instrum. 20(2), 85-94.

Mewis J. and Moldenaers P. (1999): Rheometry of complex fluids, Korea-Aust Rheol J 11(4), 313-320.

Mohtaschemi M., Dimic-Misic K., Puisto A., Korhonen M., Maloney T., Paltakari J. and Alava M. J. (2014): Rheological characterization of fibrillated cellulose suspensions via bucket vane viscometer, Cellulose 21(3), 1305-1312.

Morrison FA (2001): Understanding rheology. Oxford University Press, New York.

Naderi A. and Lindström T. (2016): A comparative study of the rheological properties of three different nanofibrillated

cellulose systems, Nordic Pulp & Paper Research Journal 31(3), 354-363.

Nechyporchuk O., Belgacem M. N. and Pignon F. (2014): Rheological properties of micro-/nanofibrillated cellulose suspensions: wall-slip and shear banding phenomena, Carbohydr. Polym. 112, 432-439.

Ouriev B. and Windhab E. J. (2002): Rheological study of concentrated suspensions in pressure-driven shear flow using a novel in-line ultrasound Doppler method, Exp. Fluids 32(2), 204-211.

Pettersson A. J., Wikström T. and Rasmuson A. (2006): Near wall studies of pulp suspension flow using LDA, Can. J. Chem. Eng. 84(4), 422-430.

Powell R. L. (2008): Experimental techniques for multiphase flows, Phys. Fluids 20(4), 040605-040605-22.

Powell R. L., Maneval J. E., Seymour J. D., McCarthy K. L. and McCarthy M. J. (1994): Nuclear magnetic resonance imaging for viscosity measurements, J. Rheol. 38(5), 1465-1470.

Raynaud J., Moucheront P., Baudez J., Bertrand F., Guilbaud J. and Coussot P. (2002): Direct determination by nuclear magnetic resonance of the thixotropic and yielding behavior of suspensions, J. Rheol. 46(3), 709-732.

Ricci S., Liard M., Birkhofer B., Lootens D., Bruhwiler A. and Tortoli P. (2012): Embedded Doppler system for industrial in-line rheometry, IEEE Trans. Ultrason. Ferroelectr. Freq. Control 59(7), 1395-1401.

Saarinen T., Haavisto S., Sorvari A., Salmela J. and Seppälä J. (2014): The effect of wall depletion on the rheology of microfibrillated cellulose water suspensions by Optical Coherence Tomography, Cellulose 21(3), 1261-1275.

Salmela J., Haavisto S., Koponen A., Jäsberg A. and Kataja M. (2013): Rheological characterization of micro-fibrillated cellulose fibre suspension using multi scale velocity profile measurements, Transactions of the 15th fundamental research symposium, Cambridge, UK, September, 2013, The Pulp and Paper Fundamental Research Society, ,495-509.

Schmitt J. M. (1999): Optical Coherence Tomography (OCT): a review, IEEE Journal on Selected Topics in Quantum Electronics 5(4), 1205-1215.

Shafiei-Sabet S., Martinez M. and Olson J. (2016): Shear rheology of micro-fibrillar cellulose aqueous suspensions, Cellulose 23(5), 2943-2953.

Soszynski R. (1991): The plug flow of fiber suspensions in pipes. A case of clear water annulus, Nordic Pulp and Paper Research Journal 6(3), 110-117.

Sumida M. (2013): Flow Properties of Wood Pulp Suspensions in Pipes, World Academy of Science, Engineering and Technology, International Journal of Mechanical, Aerospace, Industrial, Mechatronic and Manufacturing Engineering 7(11), 2202-2206.

Szkulmowska A., Szkulmowski M., Kowalczyk A. and Wojtkowski M. (2008): Phase-resolved Doppler optical coherence tomography-limitations and improvements, Opt. Lett. 33(13), 1425-1427.

Tatsumi D., Ishioka S. and Matsumoto T. (2002): Effect of Fiber Concentration and Axial Ratio on the Rheological Properties of Cellulose Fiber Suspensions. J. Soc. Rheol. Jpn., 30(1), 27-32.

Wang R. K. (2004): High-resolution visualization of fluid dynamics with Doppler optical coherence tomography, Measurement Science and Technology 15(4), 725-733.

Wang X., Milner T., Chen Z. and Nelson J. (1997): Measurement of fluid-flow-velocity profile in turbid media by the use of optical Doppler tomography, Appl. Opt. 36(1), 144-149.

Wassell P., Wiklund J., Stading M., Bonwick G., Smith C., Almiron□Roig E. and Young N. W. (2010): Ultrasound Doppler based in□line viscosity and solid fat profile measurement of fat blends, Int. J. Food Sci. Tech. 45(5), 877-883.

Wunderlich T. and Brunn P. (2000): A wall layer correction for ultrasound measurement in tube flow: comparison between theory and experiment, Flow Meas. Instrum. 11(2), 63-69.

Wunderlich T. and Brunn P. O. (1999): Ultrasound pulse Doppler method as a viscometer for process monitoring, Flow Meas. Instrum. 10(4), 201-205.

Manuscript received April 10, 2017
Accepted September 20, 2017